available at www.sciencedirect.com

SCIENCE DIRECT®

journal homepage: www.elsevier.com/locate/ecolmodel

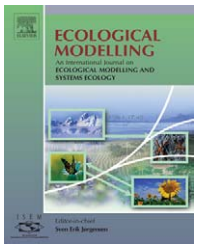

Spatio-temporal community dynamics induced by frequency dependent interactions

Margaret J. Eppstein[a,*], *James D. Bever*[b], *Jane Molofsky*[c]

[a] *Department of Computer Science, University of Vermont, 327 Votey Bldg., 33 Colchester Ave., Burlington, VT 05405, USA*
[b] *Department of Biology, Indiana University, Bloomington, IN 47405, USA*
[c] *Department of Botany, University of Vermont, Burlington, VT 05405, USA*

ARTICLE INFO

Article history:
Received 31 May 2005
Received in revised form
4 January 2006
Accepted 9 February 2006
Published on line 19 April 2006

Keywords:
Frequency dependence
Spatial models
Cellular automata
Community dynamics
Coexistence
invasiveness

ABSTRACT

A mathematical model incorporating the effects of possibly asymmetric frequency dependent interactions is proposed. Model predictions for an idealized two-species annual plant community with asymmetric linear frequency dependence are explored using (i) analytic mean field equilibrium predictions, (ii) deterministic, discrete-time, finite-population, mean field predictions, and (iii) stochastic, discrete-time, cellular automata predictions for a variety of sizes of the spatial interaction and dispersal neighborhoods. We define species interaction factors, ranging from 0 to 1, which incorporate both frequency independent and frequency dependent terms. The maximum competitive ability of a species is reduced unless species frequency is optimal based on species-specific frequency dependence coefficients, ranging from −1 to +1. Assuming that maximum competitive ability is identical for two species, they can coexist indefinitely when they have equal absolute magnitude or both have sufficiently negative frequency dependence. Although smaller scales of spatial interactions reduce the region of the parameter space in which stable coexistence is predicted, the time to extinction of one species can be significantly increased or decreased by the locality of interactions, depending on whether the losing species has positive or negative frequency dependence, respectively. The sensitivity to initial conditions in the community at large is dramatically reduced as the spatial scale of interactions is decreased. As a consequence, smaller spatial interaction neighborhoods increase the ability of introduced species to invade established communities in regions of the parameter space not predicted by mean field approximations. In the "loser positive, winner positive" regions, smaller scales of interaction dramatically increased invasiveness. In the "loser positive, winner negative" regions of the parameter space, invasion success decreases, but time to extinction of the resident species during successful invasions increases, with an increase in the spatial scale of interactions. The "loser negative, winner positive" regions were relatively insensitive to initial conditions, so invasion success was relatively high at a variety of spatial scales. Surprisingly, invasions in parts of this region are most often successful with intermediate neighborhood sizes, although the maximum time that the losing species could persist before being driven to extinction increases with an increase in the spatial scale of interactions. These results

* *Corresponding author*. Tel.: +1 802 656 1918; fax: +1 802 656 0696.
E-mail address: Maggie.Eppstein@uvm.edu (M.J. Eppstein).

0304-3800/$ – see front matter © 2006 Elsevier B.V. All rights reserved.
doi:10.1016/j.ecolmodel.2006.02.039

are explained by understanding cluster formation and density and the relative local inter-specific dynamics in cluster interiors, exteriors, and boundaries. In summary, frequency dependent interactions, and the spatial scale on which these interactions occur, can have a big impact on spatio-temporal community dynamics, with implications regarding species coexistence and invasiveness. The model proposed herein provides a theoretical framework for studying frequency dependent interactions that may shed light on spatio-temporal dynamics in real ecological communities.

© 2006 Elsevier B.V. All rights reserved.

1. Introduction

Competitive interactions abound in the natural world, and these have historically been considered one of the major organizing principles in ecological communities. Consequently, there is a rich body of literature developing a theoretical framework for the study of competitive interactions (e.g., Volterra, 1926; Lotka, 1932; Tilman, 1982, 1994; Pacala and Levin, 1997; Neuhauser and Pacala, 1999; Chesson, 2000). These models manifest negative density dependence, as populations compete for finite resources in the environment. Species coexistence in these resource-governed models requires niche divergence, wherein direct inter-specific competition is reduced and species limit themselves more than they limit other species. Hubbell (2001) argues that ecologically equivalent species can coexist over long time intervals, although ecological drift will eventually cause extinctions unless counterbalanced by migration. In Hubbell's neutral model, recruitment into the community is proportional to the relative abundance of species at some spatial scale.

There are also many examples of positive or negative frequency (or density) dependent spatial interactions that are not caused by competition for a pre-existing finite pool of resources (Clarke, 1969; Connell, 1983; May and Anderson, 1983; Condit et al., 1992; Wilson and Agnew, 1992; Ronsheim, 1996; Smithson and McNair, 1996; Holmgren et al., 1997; Bever, 1999; Weltzin and McPherson, 1999; Catovsky and Bazzaz, 2000; Harms et al., 2000; Reinhart et al., 2003; Callaway et al., 2004). Such interactions affect growth and reproduction, and therefore ultimately affect relative competitive abilities, of species in ecological communities. In experimental communities of annual and biennial plants, relative competitive abilities of four naturally co-occurring plant species were shown to be differentially positively or negatively affected by aggregation of con-specifics, thereby promoting community diversity (Stoll and Prati, 2001). Negative frequency dependence is often cited as a mechanism for the maintenance of diversity in ecological communities (Wills et al., 1997; Wills and Condit, 1999; Harms et al., 2000; Chesson, 2000; Wright, 2002; Bever, 2003). Interactions that occur through intermediaries such as through pollinators (Ågren, 1996; Smithson and McNair, 1996) or mycorrhizae (Ronsheim, 1996; Bever et al., 1997; Ronsheim and Anderson, 2001; Bever, 2002) and/or through predators (Clarke, 1969) or pathogens (May and Anderson, 1983; Westover and Bever, 2001) often create frequency dependent interactions. For example, subsurface communities of symbiotic mycorrhizae may flourish near certain species, rendering the soil more favorable to growth of others of the same species (positive frequency dependence). Conversely, accumulation of species-specific soil pathogens can increase seedling mortality in the area (negative frequency dependence).

Because spatial structure in communities can have dramatic impacts on plant community dynamics (Czárán and Bartha, 1992; Herben et al., 2000), there has been an increasing recognition of the need for spatially explicit models of ecological interactions (Balzter et al., 1998; Berec, 2002; Wu and Marceau, 2002). Spatially explicit formulations of Lotka–Volterra competition models have shown that changing the scale of spatial interactions in homogeneous environments alters the region of the parameter space where coexistence at equilibrium can be achieved (Neuhauser and Pacala, 1999; Murrell et al., 2002). Spatial heterogeneity of resources can clearly increase community structure and diversity. However, in many cases environmental heterogeneity may actually be internally generated (or augmented) through ecological feedbacks (Czárán and Bartha, 1992; Herben et al., 2000; Bascompte and Rodríguez, 2000; Feagin et al., 2005). There is a growing body of evidence that frequency dependent effects mediated by both biotic and abiotic changes to the subsurface environment may play an important role in invasiveness by exotic plant species, and must be understood and considered for effective conservation and restoration of plant communities (Wolfe and Klironomos, 2005).

Recently, some spatially explicit models have begun to elucidate the importance of frequency or density dependent effects on spatio-temporal dynamics in plant communities. In a single species model with an Allee effect (positive intra-specific density dependence at low frequencies), the ability of small local initial adult distributions to establish and persist was shown to be very sensitive to the shape of the dispersal kernel (Etienne et al., 2002). Feagin et al. (2005) found that both an external environmental gradient and facilitative succession (positive inter-specific frequency dependence) were required in order to accurately simulate community organization in a sand dune plant community. Wang et al. (2003) found a non-linear response between weed control and weed patch size, due to implicit "aggregation effects" of large patches that made weeds inside patches more resistant to external controls. More generally, Molofsky et al. have examined how community structure is affected by the spatial scale and strength of symmetric frequency dependent interactions, both negative (Molofsky et al., 2002) and positive (Molofsky et al., 2001; Molofsky and Bever, 2002). For example, they have shown that positive intra-specific frequency dependence can promote stable coexistence of species through the formation of single-species clusters, if the interactions are spatially localized. Their models assume that the magnitude and direction of frequency dependence is identical for all species in the

community, which is unlikely to be the case for any real community.

In this paper, we extend the general theoretical framework for examining the effects of positive or negative frequency dependent interactions to communities in which the strength and/or sign of these interactions may differ for each species. We develop predictions of the proposed model for idealized two-species communities of annual plants based on analytical mean field stability analysis, deterministic finite-population mean field simulations, and spatially explicit stochastic cellular automata simulations. Through these models, we explore the interplay between the magnitude, direction, and spatial scale of linear intra-specific frequency dependent interactions, and how such interactions will affect community dynamics. While future work will extend our analysis to include non-linear interactions, inter-specific frequency dependence, species-specific differences in maximum habitat suitability, and multiple species, herein we explore the spatial and temporal dynamics of species extinction, coexistence, and invasiveness in various regions of the frequency dependence parameter space for two species with equal maximum competitive abilities and species-specific intra-specific frequency dependence.

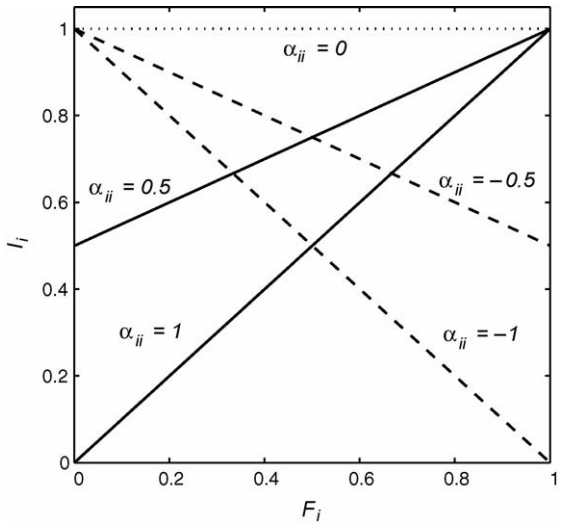

Fig. 1 – The linear frequency dependence interaction factor I_i for species i as a function of frequency of species i (Eq. (2.3)), shown for five representative values of frequency dependence α_i.

2. Model development

2.1. *Deterministic mean field model*

For simplicity, we consider a two-species community of annual plants in which the only competitive interaction is for space, and where plants of each species require the same amount of space to grow. The degree to which each species is suited to the habitat is capped by a frequency independent maximum $\beta_i \geq 0$, but can be modified downward by a frequency dependent interaction factor $I_i^t \in [0, \ldots, 1]$, based on feedbacks with the environment. Note that we denote species by subscript and time by superscript. The time varying habitat suitability H_i^t for a given species is then simply the product:

$$H_i^t = \beta_i I_i^t \tag{2.1}$$

We assume that the number of seeds of species i available for germination at time $t+1$ is directly proportional to species density D_i^t at time t. The expected relative community-wide frequency F_i^{t+1} of each species i at time $t+1$ can be determined, based on their relative products of habitat suitability and prevalence $H_i^t D_i^t$, by the following discrete-in-time approximation:

$$F_i^{t+1} = \frac{H_i D_i^t}{H_1 D_1^t + H_2 D_2^t} \tag{2.2}$$

When individuals of each species are equal competitors ($H_1^t = H_2^t$), Eq. (2.2) predicts that current population frequencies will be maintained, whereas a species with a higher habitat suitability factor will increase in relative frequency. The functional form of the interaction factors I_i will depend on the nature of the particular feedback interactions. In reality, there may be several different but simultaneous types of interactions within and between various species. If these interactions operate via the same intermediary, then they would be additive. However, if multiple interactions are independent of each other, for example operating at different periods in the life history of the plants, then their effects could be multiplicative. Here, we consider a single type of simple linear intra-specific frequency dependence, where the interaction factor is defined as follows:

$$I_i^t = \begin{cases} 1 - \alpha_{ii} + \alpha_{ii} F_i^t, & \text{if } \alpha_{ii} > 0 \\ 1 + \alpha_{ii} F_i^t, & \text{if } \alpha_{ii} \leq 0 \end{cases} \tag{2.3}$$

where α_{ii} is a parameter ranging from −1 to +1 and represents the degree to which the habitat suitability for species i is negatively or positively affected by the frequency of species i in the community. Eq. (2.3) is graphed in Fig. 1, and illustrates the decline in habitat suitability at sub-optimal frequencies, for different representative frequency dependence coefficients α_{ii}.

A previously proposed model for representing symmetric frequency dependent interactions in a two species annual plant community is as follows (Molofsky et al., 2001; Molofsky and Bever, 2002):

$$H_i^t = 0.5 + \gamma_{ii}(F_i^t - 0.5) \tag{2.4}$$

where γ_{ii} is also a frequency dependence parameter ranging from −1 to +1. However, in Eq. (2.4) the average habitat frequency (averaged over all possible frequencies) is assumed to always be 0.5, and the maximum habitat suitability is dependent on γ_{ii}, as follows:

$$H_i^t \leq \frac{1 + |\gamma_{ii}|}{2}, \tag{2.5}$$

whereas in Eq. (2.1) the maximum habitat suitability is governed by the independent variable β_i. Thus, Eq. (2.4) can only sample a subset of the parameter space represented by Eqs.

(2.1) and (2.3). In Molofsky et al. (2001) and Molofsky and Bever (2002), Eq. (2.4) was applied to two-species communities with symmetric frequency dependence (e.g., $\gamma_{11} = \gamma_{22}$), so both average and maximum habitat suitability were also implicitly species symmetric. However, Eq. (2.4) cannot be applied for predicting population dynamics where frequency dependence and maximum habitat suitability need to be independently varied. Eqs. (2.1) and (2.3) thus generalize and extend the situations in which frequency dependent interactions can be modeled, beyond the previously proposed theory expressed in Eq. (2.4). In order to focus on population dynamics caused by asymmetric frequency dependent effects, we apply Eqs. (2.1) and (2.3), assuming that all species have identical maximum habitat suitabilities ($\beta_i = 1$) achieved at their optimal frequencies, in all model results presented herein.

2.1.1. *Mean field stability analysis*

Because the interaction function given in Eq. (2.3) is not continuous, we analyze each of the four quadrants of the $\alpha_{11} \times \alpha_{22}$ parameter plane separately. We hereafter denote these as the ++, +−, −+, and −− quadrants, based on the sign of α_{11} and α_{22}, respectively, as illustrated in Fig. 2a.

In the ++ quadrant, there exists an internal neutral equilibrium for species i, given by:

$$F_i^{\infty} = \frac{\alpha_{ii}}{\alpha_{11} + \alpha_{22}} \tag{2.6}$$

Analysis of local stability (Edelstein-Keshet, 2005) indicates that this internal equilibrium is unstable, while the two trivial equilibria ($F_i^{\infty} = 0, F_i^{\infty} = 1$) are stable. This implies that stable fixation of either species is possible depending upon initial conditions (i.e., positive frequency dependent reinforcement). Specifically, the neutral equilibrium line separating the two stable equilibria (Fig. 2b) has slope C, which is dependent on initial conditions. For the mean field approximation, this slope is simply the ratio of the initial frequency of the two species, as follows:

$$C_{\text{mean field}} = \frac{F_1^0}{F_2^0}, \tag{2.7}$$

and coexistence is predicted in the ++ quadrant by the analytic mean field model only when:

$$\frac{\alpha_{11}}{\alpha_{22}} = \frac{F_1^0}{F_2^0}. \tag{2.8}$$

In the −− quadrant an internal equilibrium also exists for two species i and j, $i \neq j$, given by:

$$F_i^{\infty} = \frac{\alpha_{jj}}{\alpha_{11} + \alpha_{22}} \tag{2.9}$$

Analysis of local stability indicates that this internal equilibrium is stable while the two trivial equilibria ($F_i^{\infty} = 0, F_i^{\infty} = 1$) are unstable. This implies that the two species will coexist indefinitely, the expected result with negative frequency dependence (Fig. 2c).

In considering the −+ and +− quadrants, the two species will have equal fitness when $\alpha_{11} = -\alpha_{22}$, independent of their initial frequencies, and therefore their relative abundance will neutrally drift under this condition. Besides this special case, there is no internal equilibrium. Above the $\alpha_{11} = -\alpha_{22}$ line one

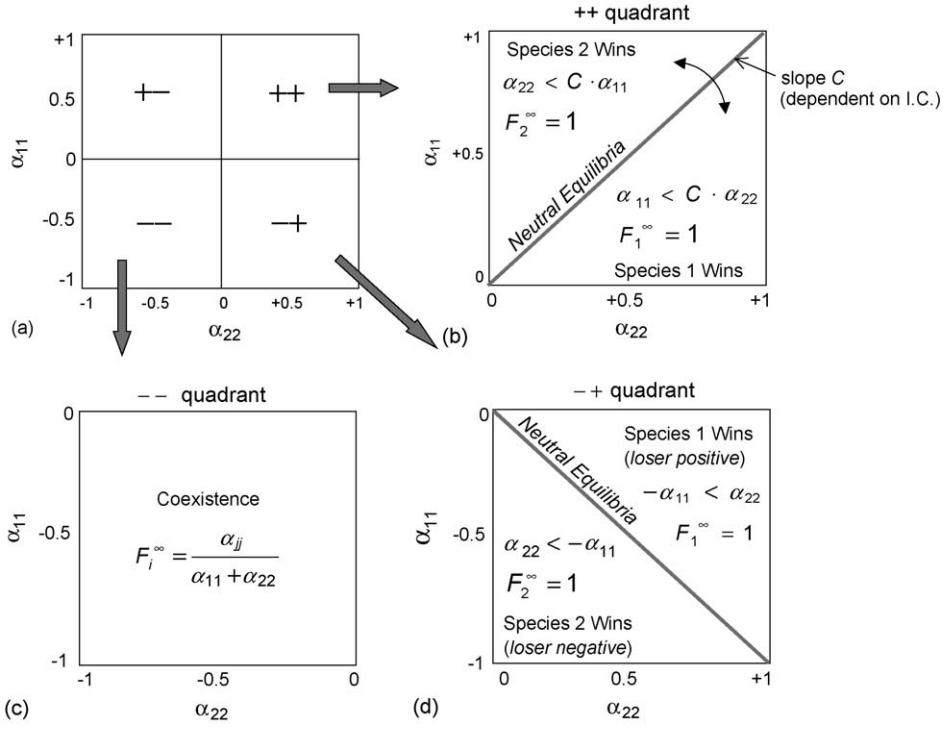

Fig. 2 – (a) Quadrant map for the $\alpha_{11} \times \alpha_{22}$ parameter space. Analytic mean field stability analysis predictions for: (a) +− quadrant, (b) ++ quadrant, and (c) −− quadrant. A quadrant map is shown in (d) for reference. The −+ quadrant (d) is symmetric with the +− quadrant shown in (a).

species will dominate and below the line the other will dominate (as illustrated for the $-+$ quadrant in Fig. 2d; the $+-$ is symmetric with this and is therefore not explicitly shown).

2.1.2. *Deterministic mean field model predictions*

We implemented a deterministic mean field model for a finite population of 100,000 annual plants to make predictions across the entire $\alpha_{11} \times \alpha_{22}$ parameter plane (in frequency dependent increments of 0.1). The deterministic mean field model comprises a Matlab 7.0 implementation of Eqs. (2.1)–(2.3) (where density predictions were based on frequencies then rounded to whole individuals) embedded within a loop that steps through time until the predictions converge. In Fig. 3a, we illustrate model results when $F_1^0 = F_2^0$. Here, black denotes regions where species 1 "wins" (drives species 2 to extinction), white denote regions where species 2 wins, and grayscale indicates the relative proportions of the two species in regions where coexistence is predicted. In regions where one species dominates over the other, the species with the lower absolute frequency dependence is the winner. In retrospect this result is obvious, because species with lower absolute frequency dependence have fewer constraints on which cells they can occupy and are therefore able to outcompete species with the same maximum habitat suitability but greater frequency dependence. Note that above the $\alpha_{11} = -\alpha_{22}$ line, the loser has positive frequency dependence, while below the line the loser has negative frequency dependence.

2.2. *Stochastic spatially explicit model*

Up until this point, we have presented the population growth model as a mean field model. Eqs. (2.1)–(2.3) can be made spatially explicit as follows:

$$F_i^{t+1}(\tilde{\mathbf{x}}) = \frac{\beta_i I_i^t(\tilde{\mathbf{x}})|_{\eta_i^I} D_i^t(\tilde{\mathbf{x}})|_{\eta_i^D}}{\beta_1 I_1^t(\tilde{\mathbf{x}})|_{\eta_1^I} D_1^t(\tilde{\mathbf{x}})|_{\eta_1^D} + \beta_2 I_2^t(\tilde{\mathbf{x}})|_{\eta_2^I} D_2^t(\tilde{\mathbf{x}})|_{\eta_2^D}} \tag{2.10}$$

$$I_i^t(\tilde{\mathbf{x}})|_{\eta_i^I} = \begin{cases} 1 - \alpha_{ii} + \alpha_{ii} F_j^t(\tilde{\mathbf{x}})|_{\eta_j^I}, & \text{if } \alpha_{ii} > 0 \\ 1 + F_j^t(\tilde{\mathbf{x}})|_{\eta_j^I}, & \text{if } \alpha_{ii} \le 0 \end{cases} \tag{2.11}$$

where $\tilde{\mathbf{x}}$ represents a location vector in space (e.g., $\langle x, y \rangle$ spatial coordinates), and the general notation $f_i(\tilde{\mathbf{x}})|_{\eta_i^f}$ means to evaluate the function f for species i, within a spatial neighborhood η, centered around location $\tilde{\mathbf{x}}$, where the size, shape, and weight of the neighborhood basis function is specific to species i and the function f for the application in question. The neighborhoods for non-competitive interactions (η_i^I) and dispersal (η_i^D) may be species-specific and distinct for each type of interaction.

Stochasticity may be introduced (as in Molofsky et al., 2001; Molofsky and Bever, 2002) by replacing the deterministic prediction of frequency by a stochastic prediction, wherein species i will occupy location $\tilde{\mathbf{x}}$ at time $t+1$ with probability:

$$P_i^{t+1}(\tilde{\mathbf{x}}) = F_i^{t+1}(\tilde{\mathbf{x}}) \tag{2.12}$$

where $F_i^{t+1}(\tilde{\mathbf{x}})$ is computed by Eq. (2.10). If the denominator of Eq. (2.10) is zero, then the probability in (2.12) is simply set to zero and the cell at location $\tilde{\mathbf{x}}$ is treated as empty for the next generation. If $\alpha_{ii} = 0$ and $\beta_{ii} = 1$, $\forall i$, then this probability reduces to:

$$P_i^{t+1}(\tilde{\mathbf{x}}) = \frac{D_i^t(\tilde{\mathbf{x}})|_{\eta_i^D}}{D_1^t(\tilde{\mathbf{x}})|_{\eta_1^D} + D_2^t(\tilde{\mathbf{x}})|_{\eta_2^D}} \tag{2.13}$$

i.e., in Eq. (2.13) the probability that species i will occupy the cell at $\tilde{\mathbf{x}}$ in the next generation is simply determined by its proportionate density in the neighborhood, sensu the voter model (Holley and Liggett, 1975; Hubbell, 2001). The above equations are easily extended to handle more than two species and/or non-zero inter-specific frequency dependence, but we do not report on these extensions here.

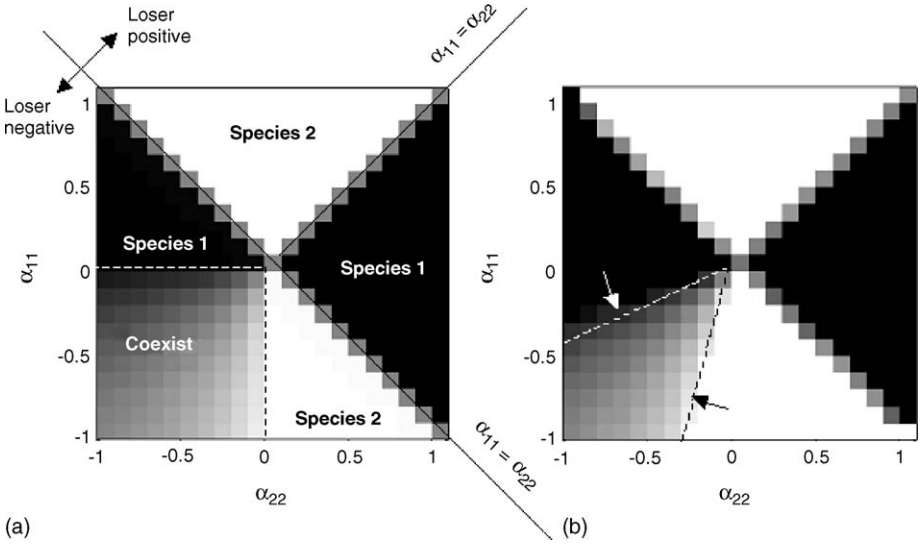

Fig. 3 – (a) Finite-population deterministic mean field and (b) 3 × 3 cell neighborhood model predictions, starting with equal proportions of each species in a striped distribution. Grayscale represents the predicted frequencies of each species, where black means 100% species 1 and white means 100% species 2.

Stochastic spatially-explicit models are implemented in Matlab v.7.0 as follows. Eqs. (2.11) and (2.12) are simulated on a Cartesian grid of discrete cells, wherein each of the discrete cells can be occupied by at most one individual from any of the species in the community. All operations are highly vectorized in Matlab to achieve computational efficiency. In the remainder of this manuscript we report on experiments for synthetic two species annual plant communities as follows. We employed 100×100 cell grids with no uninhabitable cells and non-periodic boundary conditions (i.e., with no toroidal wrap-around, so local species frequencies around cells near boundaries were simply computed over smaller neighborhoods), because these more accurately represent boundary conditions in natural communities of finite extent. Prior experimentation had shown that larger grids and use of periodic boundary conditions result in quantitative differences in time to extinction, but do not qualitatively alter relative model behavior in the different parts of the parameter space. The only competitive interaction is for space, wherein the species that occupies a given cell (wins the competition) is stochastically based on Eq. (2.12). Each species exhibits one frequency dependent interaction based on the frequency of its own species, although the strength and direction of those interactions varies independently for each species. The physical environment in the community is considered to be homogeneous, with each species equally well-adapted to it. We simulate deterministic death of these annual plants, so 100% of the cells become available at the start of each year.

In the experiments reported here, we assumed uniform and equivalent square neighborhoods of cells of a given width and centered on $\tilde{\mathbf{x}}$, for determination of both density dependent seed dispersal $D_i^t(\tilde{\mathbf{x}})|_{\eta_i^D}$ and frequency dependent interactions $I_i^t(\tilde{\mathbf{x}})|_{\eta_i^I}$ of an individual in a given cell located at position $\tilde{\mathbf{x}}$. We explored coefficients of frequency dependence (α_{11}, α_{22}) that sampled the parameter space for each combination of α_{ii} in the range $[-1, +1]$, in increments of 0.1.

It should be noted that, for most of the parameter combinations tested, all cells are typically occupied each year (with the exception of certain cases with very strong negative interactions, resulting in some cells having zero probability of being occupied by either species). Thus, since we permit at most one individual per unit area in our models, most of the simulated interactions reported here could alternatively be viewed as either frequency dependent or density dependent.

3. Coexistence studies

For coexistence studies, the community was initialized with equal frequencies of the two species; i.e., $F_1^0 = F_2^0$. We explored both a "striped" initial distribution, where the left half of the environment was initially fully populated by species 1 and the right half was initially populated by species 2, and a "random" distribution, in which equal frequencies of the two species were randomly located across the domain. Although equilibrium coexistence predictions were the same from either striped or random initial distributions, the initial distribution did affect the non-equilibrium dynamics. We ran coexistence simulations for all $21^2 = 441$ possible combinations of the 21 α_{ii} coefficients $\{-1, -0.9, \ldots, 0.9, +1\}$ using the spatially-explicit stochastic model with both 3×3 cell and 100×100 cell neighborhood sizes. For consistency, this set of experiments (reported on in Figs. 3 and 4) all started from the striped initial distribution. We refer to models run with 100×100 cell neighborhoods as stochastic mean field models, since interactions are community-wide. Additional selected experiments (reported on in Fig. 5), starting from the random distribution, were run and are reported on for other neighborhood sizes in order to more clearly elucidate pattern formation and trends relating to the spatial scale of interactions. All simulations were run until either one species went extinct or for a maximum of 2000 generations (years). Prior experimentation with up to 10,000 generations had shown that results did not significantly differ from the 2000 generation predictions.

Predictions of the deterministic mean field model for the coexistence studies are shown in Fig. 3a. The stochastic mean

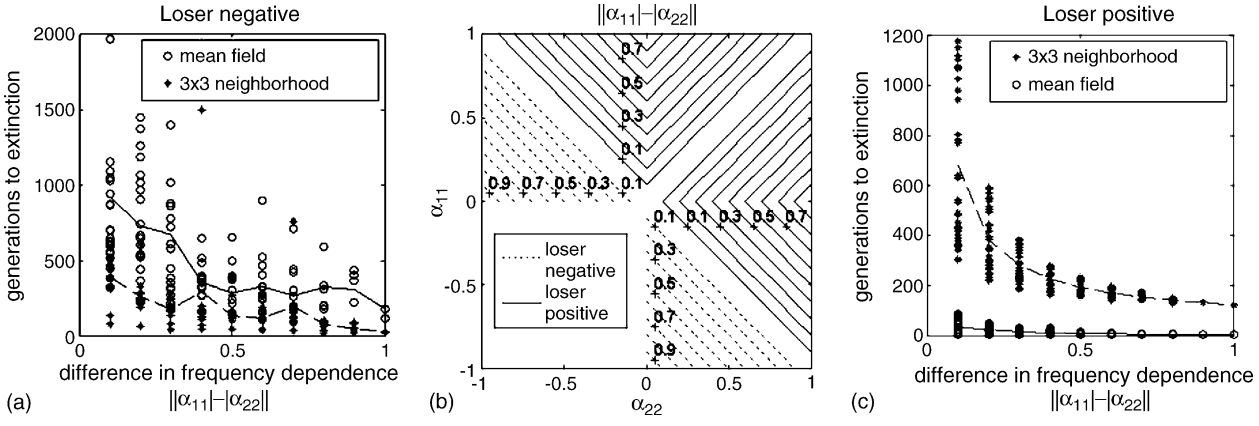

Fig. 4 – Non-equilibrium dynamics starting from a striped initial distribution. (a) Time to extinction events in the loser negative regions as a function of neighborhood size; *x*-ticks correspond to the dashed iso-difference contours ($||\alpha_{11}| - |\alpha_{22}||$) shown in (b). (c) Time to extinction events in the loser positive regions as a function of neighborhood size; *x*-ticks correspond to the solid iso-difference contours shown in (b). In (a) and (c) the dashed lines represent the average of the 3 × 3 cell neighborhood predictions and the solid lines represent the average of the stochastic mean field predictions.

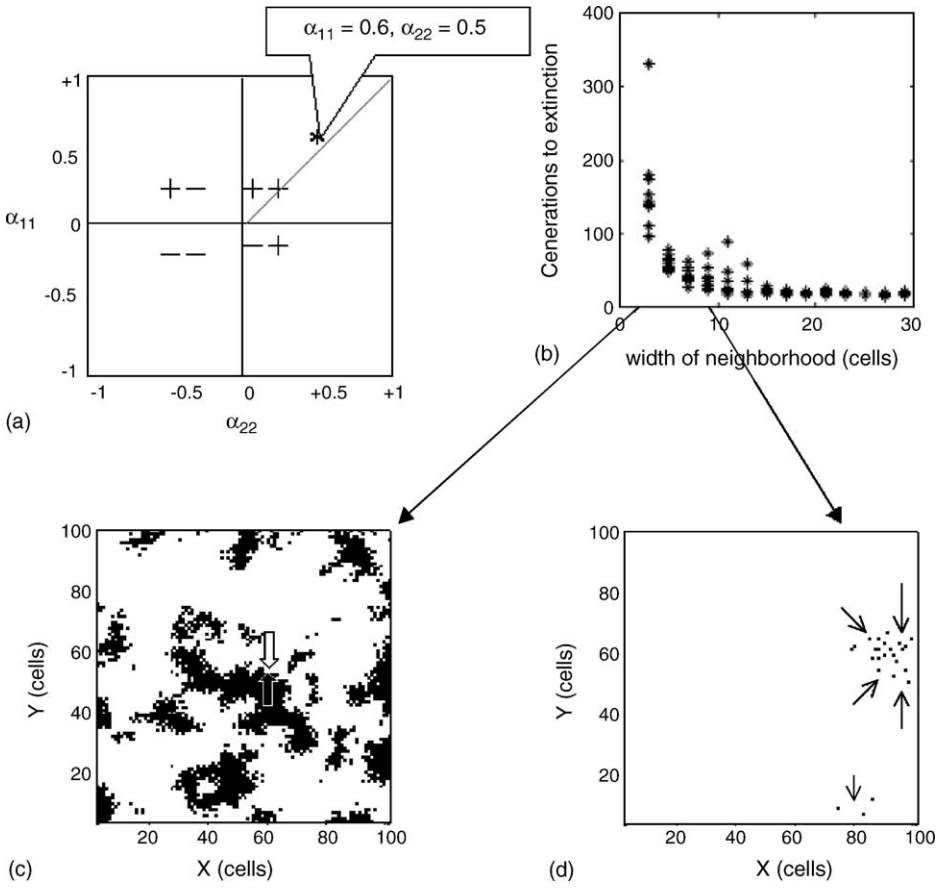

Fig. 5 – (a) The representative location $\alpha_{11} = 0.6$, $\alpha_{22} = 0.5$ in the ++ quadrant, (b) the time scale of extinction at the representative location as a function of neighborhood size, (c) a representative pattern of tight clusters of species 1 (black) shown at generation 20 of one 3 × 3 cell neighborhood simulation; the arrows represent competing forces at the cluster boundaries that help the clusters to persist, and (d) a representative pattern of loose clusters of species 1 (black) shown at generation 20 of one 9 × 9 cell neighborhood simulation, shortly before species 1 went extinct; the arrows illustrate the rapid shrinkage of these clusters. All data in this figure is starting from a random initial distribution.

field predictions (not shown) appear nearly identical to Fig. 3a, with the exception that coexistence is no longer predicted along the $\alpha_{11} = \alpha_{22}$ line in the ++ quadrant because, in the stochastic model when frequency dependence is positive and symmetric, drift ultimately always enables one species or the other to gain an advantage and drive the other to extinction. In addition, the number of generations until extinction events anywhere in the parameter plane is generally shorter in the stochastic than in the deterministic model.

When spatial interactions are limited to 3×3 cell neighborhoods, the equilibrium predictions appear similar to the stochastic mean field predictions, with the exception that the region of coexistence in the −− quadrant shrinks (Fig. 3b). This is consistent with the findings of Neuhauser and Pacala (1999) for spatial Lotka–Volterra competitive interactions where intra-specific competition is stronger than inter-specific competition. Such competitive interactions exhibit negative–negative density dependence and so behave similarly to negative–negative frequency dependent interactions. Unlike in the stochastic mean field model, the 3×3 cell neighborhood stochastic model does predict coexistence (for at least 2000 generations) along the $\alpha_{11} = \alpha_{22}$ line in the ++ quadrant. This is because the equal and positive frequency dependence of both species results in the formation of semi-stable clusters that promote coexistence. This confirms the prior findings of Molofsky and Bever (2002) using the similar model embodied in Eq. (2.4).

The apparent similarity of the equilibrium frequency predictions shown in Fig. 3a and b, for the deterministic mean field and stochastic 3×3 cell neighborhood spatially explicit models, respectively, is somewhat misleading. This is because both community structure and the time scale for the extinction events vary dramatically as a function of the spatial scale of interactions, and vary in different ways for different parts of the parameter space, as follows.

In the "loser negative" regions (below the $\alpha_{11} = -\alpha_{22}$ line in the +− and −+ quadrants), the average time to extinction decreases from an average of 548 generations in the stochastic mean field model to an average of 208 generations in the model with 3×3 cell neighborhoods. In either case, time to extinction in these regions is inversely proportional to the absolute difference in the frequency dependence of the two species ($||\alpha_{11}| - |\alpha_{22}||$), as shown in Fig. 4a, where time to extinction is plotted as a function of this difference. Note that the data

points in Fig. 4a correspond to observed numbers of generations prior to extinction along the dashed iso-difference contours in the loser negative regions shown in Fig. 4b. Although the trend is noisy, the time to extinction is generally faster for the 3×3 cell neighborhoods (asterisks and dashed line, Fig. 4a) than in the stochastic mean field model (open circles and solid line, Fig. 4a). This is because small local neighborhoods have higher apparent frequencies of the lower frequency species, so when the losing species has negative frequency dependence it is at an even greater relative disadvantage when the neighborhood size is small, and consequently the species that is less frequency dependent dominates more quickly.

In contrast, in the "loser positive" regions (above the $\alpha_{11} = -\alpha_{22}$ line) this trend is reversed. Here, the number of generations to extinction events increases from an average of 19 generations in the stochastic mean field model to an average of 326 generations (starting from a "striped" distribution) in the stochastic model with the 3×3 cell neighborhoods. When plotted as a function of difference in absolute frequency dependence (corresponding to the solid iso-difference contour lines shown in Fig. 4b), the time to extinction drops exponentially as a function of the absolute difference in frequency dependence, and is dramatically slower with small neighborhoods (asterisks and dashed line, Fig. 4c) than in the stochastic mean field model (open circles and solid line, Fig. 4c).

We further elucidate the effect of neighborhood size on time to extinction in the loser positive region by closer examination at one representative location with a small difference in frequency dependence (Fig. 5a). In Fig. 5b, we plot time to extinction as a function of neighborhood size, for 10 stochastic simulations at each of a variety of neighborhood sizes starting from a "random" equal distribution of the two species. Time to extinction is seen to drop exponentially as a function of neighborhood size (Fig. 5b). This is because smaller interaction neighborhoods facilitate the formation and retention of protective clusters of positive intra-specific frequency dependent species, offsetting small frequency dependence disadvantages and enabling them to coexist for hundreds or even thousands of generations with the less frequency dependent species that is predicted to dominate. For example, consider the tight clusters of species 1 (black), shown at generation 20 of one representative 3×3 neighborhood simulation in Fig. 5c. In this example, both species have positive frequency dependence, so in the interior of the clusters of species 1 the environment is more favorable to species 1, and individuals of species 2 are out-competed there. However, at the cluster boundaries where frequencies are roughly 50/50 within the small local neighborhoods, conditions are relatively more favorable for species 2 because this border frequency is above the critical value (Eq. (2.6)) necessary for majority advantage. Thus, the clusters of species 1 are slowly eroded at the boundaries and species 2 ultimately wins, although this may take hundreds of generations, especially if initial clumping is present (as in the "striped" initial distribution). For larger neighborhood sizes, the percent of each cluster that acts as erodable boundary is also larger, so clusters degrade more rapidly. For example, Fig. 5d shows that by generation 20 of one representative 9×9 neighborhood simulation, the very loose clusters of species 1 (black) are already nearly obliterated. At neighborhoods greater than about 12×12 cells, the clusters are so loose as to offer no protective local environment, so extinctions proceed as rapidly as in the stochastic mean field model (Fig. 5b).

4. Invasion studies

For invasiveness studies, the community was initially fully populated by species 1. Then, at the start of the simulation, various numbers of individuals from species 2 were randomly placed in the domain, such that initial ratio of species 1 to species 2 ranged from approximately 2:1 to 10,000:1. In the last case, a single individual of species 2 was placed near the center of a community fully populated by species 1. We ran invasiveness studies for the same $21^2 = 441$ possible combinations of the 21 α_{ii} coefficients $\{-1, -0.9, \ldots, 0.9, +1\}$ using the deterministic mean field model, the stochastic mean field model, and the stochastic 3×3 cell neighborhood model. The converse case (where species 1 invades species 2) was not explicitly considered since the results are symmetric. When maximum habitat suitability is equal for all species (as they are in experiments here), invasion will only be possible in those regions of the parameter space in which the invading species has a frequency dependence advantage; i.e., has the lower absolute value of frequency dependence.

The analytic mean field predictions indicated that, in the ++ quadrant, the slope of the line separating the regions in which each species would dominate should be linearly dependent on the ratio of initial frequencies of the two species (Eq. (2.7)). This result was confirmed by the predictions of both the deterministic and stochastic mean field models (although the results of the latter were obviously noisier due to random perturbations). However, when the neighborhood size was reduced to 3×3 cells, the dependence of the slope C was approximately logarithmic in the ratio of the initial community-wide frequencies (Fig. 6).

In other words, with small neighborhood sizes the outcomes are much less sensitive to the initial conditions in the community at large. This has significant implications for the ability of species 2 to invade species 1 in the ++ quadrant. For example, species 2 was not able to overcome even a mild 10:1 initial frequency difference anywhere we examined in the ++ quadrant of our 10,000 individual mean field simulations. However, when the interaction neighborhood was reduced to 3×3 cells, species 2 was repeatedly able to drive species 1 to extinction above about the $\alpha_{11} = 2 \cdot \alpha_{22}$ line when starting from a 100:1 initial frequency disadvantage. Even when starting with only a single individual of species 2 (a 10,000:1 initial frequency disadvantage), species 2 was occasionally able to invade in the ++ quadrant above the $\alpha_{11} = 10 \cdot \alpha_{22}$ line. The reason that smaller neighborhoods promote invasiveness in the parts of the ++ quadrant where species 2 (the invader) has a frequency dependent advantage is that the relative frequency of species 2 appears higher in small local neighborhoods than in the community at large. For example, in our study one individual of species 2 introduced into a community of 10,000 individuals of species 1 has a local frequency of 1/9 within the 3×3 cell neighborhood centered on the location of the propagule, as opposed to its community-wide frequency of 1/10,000. Thus, even a 10:1 frequency dependent advantage will favor

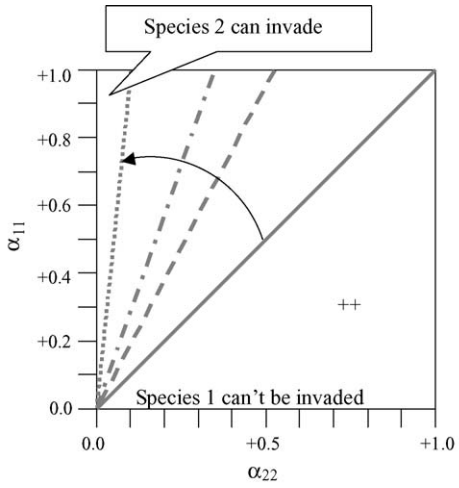

++ quadrant	Neighborhood size	
slope C of neutral equilibrium line	mean field $F_1^0 : F_2^0$	3×3 cells $F_1^0 : F_2^0$
1	1:1	1:1
2	2:1	~100:1
3	3:1	~1000:1
10	10:1	~10000:1

Fig. 6 – Sensitivity to initial conditions in the ++ quadrant as a function of neighborhood size. In the mean field model, the slope of the neutral equilibrium line is directly proportional to the initial proportions of the two species. In a 3 × 3 cell neighborhood model the relationship is approximately logarithmic in the initial proportions of the community of 10,000. Above this line species 2 will invade and drive species 1 to extinction, below the line species 1 will resist invasion.

the invader in the its local 3 × 3 cell neighborhood, and once a foothold is established the cluster of species 2 will rapidly expand and ultimately drive the more frequency dependent (resident) species extinct. As in the mean field model, the dependence on initial conditions in the ++ quadrant is linear, with slope C (recall Eq. (2.7)). However, when interactions are limited to local neighborhoods, the establishment of the introduced species, and therefore the slope C, is governed by the frequency of the neighborhood with the most introduced propagules. Without loss of generality, if we assume that species 1 is the resident species and species 2 is the introduced species, this can be formalized as the minimum relative neighborhood frequency of the resident at the time of the introduction ($t = 0$), over all local interaction neighborhoods η^{I} in the domain, as follows:

$$C_{\eta_1^{\mathrm{I}}\eta_2^{\mathrm{I}}} = \min_{\forall \tilde{\mathbf{x}}} \left(\frac{F_1^0(\tilde{\mathbf{x}})|_{\eta_1^{\mathrm{I}}}}{F_2^0(\tilde{\mathbf{x}})|_{\eta_2^{\mathrm{I}}}} \right) \tag{4.1}$$

Note that Eq. (4.1) converges to Eq. (2.7) as the size of the interaction neighborhoods η_1^{I} and η_2^{I} increase and approach the domain size. Although the analytic infinite-population mean field analysis indicated that only the ++ quadrant should be dependent on the initial conditions (Fig. 2), our experiments showed that outcomes of even the deterministic mean field finite-population models could be influenced by initial conditions across much of the $\alpha_{11} \times \alpha_{22}$ parameter plane.

For example, in the +− quadrant, the intercept of the line separating the loser positive (resident goes extinct) from loser negative (invader goes extinct) regions was observed to vary in direct proportion to the initial frequencies of the two species in the deterministic finite-population mean field model (Fig. 7), even though this quadrant is not predicted to be sensitive to initial conditions by the analytic mean field model. Above this line, species 2 was able to invade and drive species 1 to extinction (loser positive), but at or below this line the invading species 2 was not able to increase its frequency above the initial proportions, due to the discrete frequency increments in finite populations. In an infinite-population mean field model (no rounding to whole individuals), a large disadvantage in species proportions that was offset by even a small frequency dependence advantage was slowly reduced until a critical point of instability was reached, at which time the less frequency dependent species rapidly drove the other to extinction (loser negative). However, in the finite-population mean field model, predicted increases of less than 0.5 individuals were truncated to 0, with the result that the initial proportions never changed and a stable equilibrium was maintained. In the stochastic mean field model, drift always caused one or the other species to win and, although the line separating the loser positive and loser negative regions was irregular due to random events, the average percent of the +− quadrant in which the loser was positive (i.e., in which species 2 could drive species 1 to extinction) was the same as in the deterministic mean field model. Since real plant communities are finite, these deviations from the mean field predictions may lend meaningful insight on the potential of positively frequency dependent residents to resist invasion by negatively frequency dependent species that have a frequency dependence advantage, where such resistance is not predicted by the analytic mean field model.

For the same reasons as in the ++ quadrant, smaller neighborhood sizes in the +− quadrant rendered the model much less sensitive to initial conditions, with the intercept of the line separating the loser positive and loser negative regions roughly proportional to the logarithm of the ratio of initial proportions for the 3 × 3 cell neighborhoods in this 10,000 member community (Fig. 7). Even with a 10,000:1 initial frequency disadvantage, species 2 was able to occasionally invade species 1 in the +− quadrant, given a sufficiently large frequency dependence advantage. We explored the invasion dynamics in this region by closer examination of one representative point in the

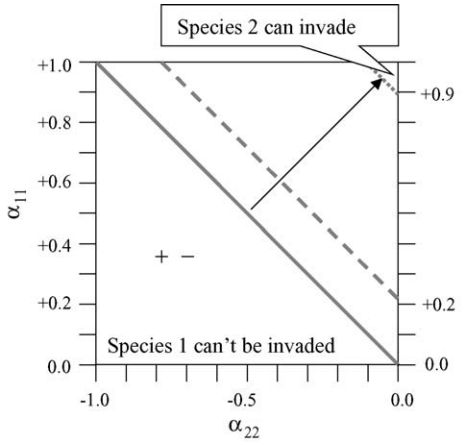

+ − quadrant	Neighborhood size	
intercept of neutral equilibrium line	discrete mean field $F_1^0 : F_2^0$	3×3 cells $F_1^0 : F_2^0$
0.0	Up to ~40:1	Up to at least 100:1
+0.2	~60:1	~1000:1
+0.9	~140:1	~10000:1

Fig. 7 – Sensitivity to initial conditions in the + − quadrant as a function of neighborhood size. In the mean field model, the intercept of the neutral equilibrium line is directly proportional to the initial proportions of the two species. In a 3 × 3 cell neighborhood model the relationship is approximately logarithmic in the initial proportions in the 10,000 member community at large. Above this line species 2 will invade and drive species 1 to extinction, below the line species 1 will resist invasion.

+ − quadrant, located at $\alpha_{11} = 0.8$, $\alpha_{22} = -0.1$ (Fig. 8a). We ran 100 simulations in which we introduced one individual of species 2 into the center of an established community of species 1, at each of a number of neighborhood sizes, and found that the percent of invasion success decreased linearly with neighborhood size ($R^2 = 0.78$), with a maximum invasion success rate of 14% for the 3 × 3 cell neighborhoods (Fig. 8b). Although invasion success was higher for small neighborhoods, the time it took for the invaders to completely overtake the resident species was generally higher for small neighborhood

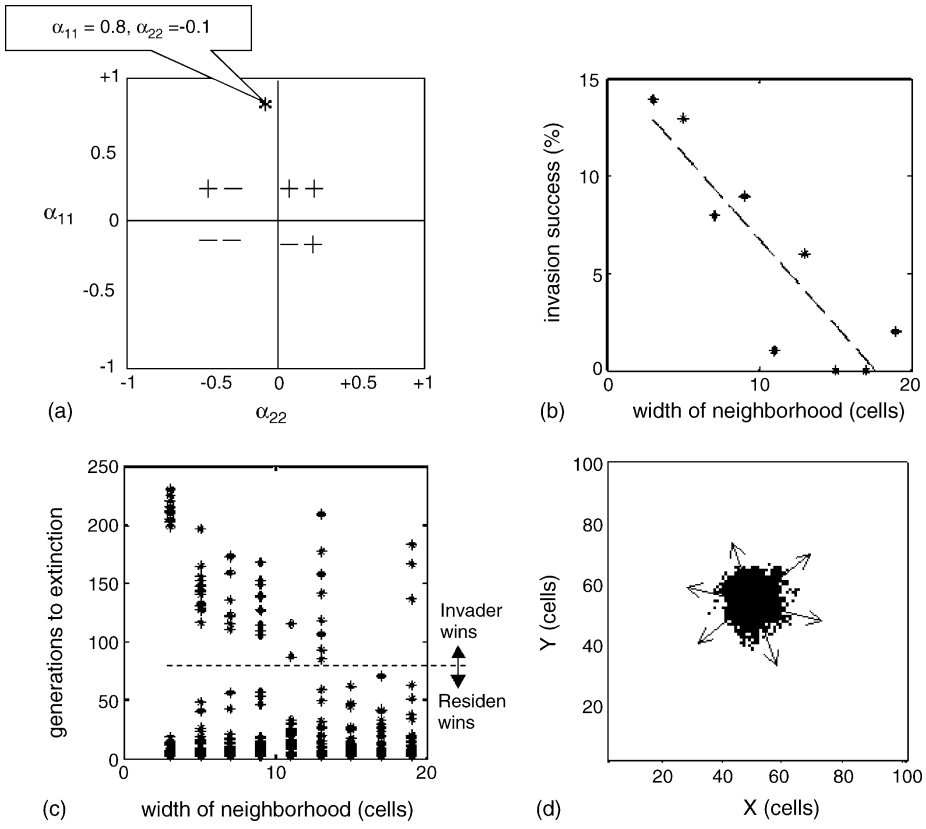

Fig. 8 – (a) The representative location $\alpha_{11} = 0.8$, $\alpha_{22} = 0.1$ in the + − quadrant, (b) invasion success as a function of neighborhood size, (c) generations to extinction events as a function of neighborhood size; above the dashed line the resident went extinct, below the dashed line the invader went extinct, and (d) one representative invading tight cluster of species 2 (black) 40 generations after the introduction of a single individual of species 2 in a 3 × 3 cell neighborhood model.

sizes (Fig. 8c). The reason for these behaviors is illustrated in Fig. 8d, which shows a representative tight expanding cluster of invaders, at generation 40 of a successful invasion event, with neighborhood size of 3 × 3 cells. As with the coexistence results, smaller spatial interactions facilitate the formation of tighter clusters. Soon after an invader is introduced, stochastic events can cause the invaders to die out before a cluster can form (Fig. 8c, below the dashed line). For the small 3 × 3 cell neighborhoods, invasive clusters become established within about 20 generations if the invading species can survive that long. For larger neighborhoods this can take up to about 80 generations. However, once a cluster of the invading species is formed, the invading species will eventually overtake the resident species. This result is somewhat counter-intuitive, because the invading species in this region has negative frequency dependence while the resident had positive frequency dependence. However, consider the dynamics at the boundary of the growing cluster of invading species 2 (black, Fig. 8d). The area just outside the cluster boundary is very favorable to species 2, because its negative frequency dependence favors occupying cells in neighborhoods where it is rare. Species 1, which has positive frequency dependence, does best in areas it previously dominated but is vulnerable at the cluster boundary. The area inside the cluster of species 2 is unfavorable to both species, but species 2 can tolerate it better than species 1 since species 2 has lower absolute frequency dependence. Consequently, once such clusters get started they grow slowly but relentlessly. Because the range of dispersal was limited to the interaction neighborhood in these simulations, the number of generations to total extinction of the resident species was highest with the smallest neighborhoods (Fig. 8c, above the dashed line).

In the loser negative region of the − + quadrant, the invasion dynamics were quite different, as illustrated in Fig. 9 for the case where $\alpha_{11} = -0.5$, $\alpha_{22} = 0.4$ (Fig. 9a). Invasion success was much higher in the loser negative region of the − + quadrant than in the loser positive region of the + − quadrant (compare Fig. 9b to Fig. 8b). This occurs because, where the established species 1 has negative frequency dependence, it is easier for individuals of the invading species 2 to avoid early extinction (Fig. 9c, below the dashed line), because the negative frequency dependence of the resident species has a tendency to make spaces available to the invader. Surprisingly, it turns out that in this case *intermediate* sized neighborhoods were the most favorable to invading species, with a maximum observed invasion success rate of 36% occurring with the 11 × 11 and 13 × 13 cell neighborhoods (Fig. 9b). We believe this non-linear relationship may occur because of the following. When neighborhood size is very small, denser clusters are formed by virtue of limited dispersal and the tendency of the positively frequency dependent invader to grow near others of its own kind. Inside dense clusters the frequency of the resident is relatively low; this is favorable to the resident, which has negative frequency dependence. Conversely, the territory outside the cluster is relatively unfavorable to the invader. This keeps the invading clusters from growing rapidly and increases the chance that stochastic events will kill off the invader before the cluster grows enough to establish a

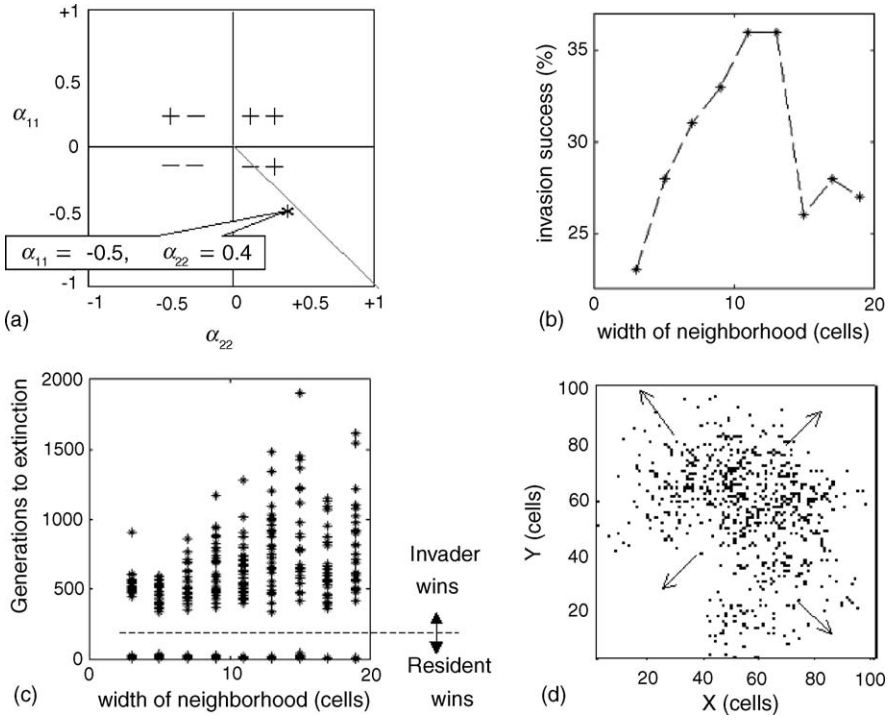

Fig. 9 – (a) The representative location $\alpha_{11} = -0.5$, $\alpha_{22} = 0.4$ in the − + quadrant, (b) invasion success as a function of neighborhood size, (c) generations to extinction events as a function of neighborhood size; above the dashed line the resident went extinct, below the dashed line the invader went extinct, and (d) one representative invading loose cluster of species 2 (black) 40 generations after the introduction of a single individual of species 2 in an 11 × 11 cell neighborhood model.

foothold on its way to dominance. On the other hand, if the spatial scale is too large, then the positively frequency dependent invaders become widely scattered early on, making them more susceptible to early stochastic die out. Thus, for this parameter combination in the loser negative region of the − + quadrant there appears to be an optimal neighborhood size for invaders that balances these two effects, as shown by the rapidly expanding loose cluster at generation 40 of one representative 11 × 11 cell neighborhood simulation, on its way to successful invasion (Fig. 9d). When a successful invasion does occur in this region, however, it proceeds more rapidly when the interaction neighborhood size is smaller (Fig. 9c, above the dashed line), i.e., although tighter clusters of invaders are more difficult to establish in this region, once they do become established they are advantageous to the invading species, which is positively frequency dependent. In comparison to the time to extinction in the loser positive region of the + − quadrant (Fig. 8c), complete extinctions take much longer in the loser negative region of − + quadrant (Fig. 9c). This is because the negative frequency dependence of the resident enables it to remain viable even when dispersed over large distances, and coexistence can occur for hundreds or even thousands of generations.

In the − − quadrant the coexistence results of all models were almost completely insensitive to initial conditions, as expected, with the exception that when there was only a single invading individual it was (i) subject to extinction by random drift in the stochastic models, and (ii) was not able to increase in frequency in the upper regions of the quadrant in the deterministic finite-population model, for the same reasons discussed with regards to the + − quadrant.

5. Discussion

Supported by a well-developed theoretical framework, much of plant ecology has focused on the importance of competition in structuring communities. However, there is growing evidence that other biotic interactions can also have important effects on plant populations, in part by generating frequency dependence in plant population growth rates. This work advances the field by developing and employing a model to explore the effects of asymmetric frequency dependent interactions at various spatial scales on the spatial and temporal dynamics of communities. As with previous investigations of local scale competition (Pacala and Levin, 1997; Neuhauser and Pacala, 1999; Bolker and Pacala, 1999; Dieckmann et al., 2000) and symmetric frequency dependence (Molofsky and Bever, 2002; Molofsky et al., 2002), we have found both qualitative and quantitative shifts in community structure resulting from the spatial scale of ecological interactions.

In the absence of drift, species that are initially equally frequent can coexist indefinitely when either (i) they have equal absolute frequency dependence or (ii) they both have sufficiently negative frequency dependence. Smaller scales of spatial interactions reduce the region of the parameter space in which indefinite coexistence is predicted. This is consistent with observations made on spatial Lotka–Volterra models (Neuhauser and Pacala, 1999), and is due to the fact that calculating frequencies over small neighborhoods has the effect of increasing the apparent frequency of the less frequent species in those neighborhoods, relative to their frequency in the community at large.

We define frequency dependent interaction factors ranging from 0 to 1, such that the maximum fitness of a species is reduced unless frequency is optimal for that species. Thus, outside of the regions where indefinite coexistence can occur, starting from equal frequencies the species with lowest absolute frequency dependence will ultimately drive the other to extinction. This result stems from the fact that less frequency dependence implies fewer constraints on which cells an individual is likely to occupy, assuming identical maximum habitat suitability. However, the dynamics of the spatial structure of the community and the resulting rate of extinction are dramatically affected by the spatial scale of the interactions. When both species have positive frequency dependence, small spatial interaction neighborhoods promote cluster formation, which in turn promotes coexistence. This is consistent with previous model outcomes for symmetric interactions (Molofsky et al., 2001; Molofsky and Bever, 2002) but extends these results to asymmetric frequency dependence. Throughout the "loser positive" regions of the parameter space (i.e., where the losing species has positive frequency dependence that is stronger than the positive or negative frequency dependence of the winning species), the time to extinction increases exponentially as the scale of spatial interactions decreases, because of the ability of the losing species to form protective clusters that stave off extinction. When two species have similar, but unequal, positive frequency dependence, they can coexist for hundreds of generations, even though mean field stability predictions indicate that one species will dominate. Conversely, in the "loser negative" regions of the parameter space (i.e., where the losing species has negative frequency dependence that is stronger than the positive frequency dependence of the winning species), the time to extinction decreases with decreasing spatial scale of interactions, because the clusters formed by the winning species can grow aggressively.

The most surprising and intriguing results, however, came from the invasiveness studies, where one or more representatives of an invading species were introduced into an established community of the other species. In these studies, the size of spatial interaction neighborhoods and the use of finite-population models dramatically affect predictions regarding how frequency dependence can potentially affect the invasiveness of species. The analytic mean field predictions indicate that when both species have positive frequency dependence, any initial disadvantage in frequency must be offset by an equally large frequency dependence advantage, if the introduced species is to successfully invade. This prediction was confirmed by the mean field cellular automata simulations, with the implication that it is virtually impossible for one species with positive frequency dependence to invade an established community of another positively frequency dependent species. However, the sensitivity to initial conditions in the community at large was dramatically reduced with decreasing spatial scale of interactions, since the species need only overcome a frequency disadvantage within

any local neighborhood in order to become established. Thus, smaller spatial interaction neighborhoods promote invasiveness when both invader and resident have positive frequency dependence, which is not predicted by mean field approximations.

When species have frequency dependence of opposite signs, the analytic mean field predicts that outcomes should be independent of initial conditions. This implies that even a single individual of a species with lower absolute frequency dependence should be able to invade and drive to extinction resident species with higher absolute frequency dependence of the opposite sign. However, our finite-population mean field and cellular automata models did not concur with this and outcomes proved sensitive to initial frequencies of the two species over these regions of the parameter space, although, as in the positive–positive case, this sensitivity to initial conditions was dramatically affected by decreasing the spatial scale of interactions. In the "loser positive, winner negative" regions of the parameter space, invasion success was inversely proportional to neighborhood size, with the smallest scales promoting the greatest invasiveness. Contrary to intuition, invaders with negative frequency dependence were able to form and exploit invasive clusters. However, the time that the losing species could persist before being driven to extinction tended to decrease with an increase in the spatial scale of interactions. The "loser negative, winner positive" regions were, in general, less sensitive to initial conditions. Surprisingly, invasions in at least part of this region were more often successful with intermediate neighborhood sizes, although the maximum time that the losing species could persist before being driven to extinction increased with an increase in the spatial scale of interactions.

The invasion results have important implications for understanding the establishment of new species into resident communities. Specifically, our results provide insights into why a small population of alien species can invade and dominate a resident plant community. The interplay between the signs of the feedback and the size of the interaction neighborhood dramatically affect both the ability of an introduced species to become established and the speed with which an established introduced species increases in frequency. Our results show that, while mean field predictions suggest that positive frequency dependence in an introduced species would inhibit their establishment in a community of positively frequency dependent natives, when frequency dependence occurs locally, as would be the case for soil feedback (Bever, 2003), introduced species may become established under much broader conditions. Once established, an invader with positive frequency dependence can overtake the resident species more quickly than when the invader has negative frequency dependence. We also demonstrate theoretically that negative frequency dependence in a resident community fosters early establishment of an introduced species, but whether the introduced species becomes invasive depends on the relative sign and strength of frequency dependence in the introduced species. Recent literature has shown that some invasive species may have undergone a shift in their interactions with their soil community from negative feedback (implying negative frequency dependence) in their native habitat to positive feedback (implying positive frequency dependence) in the new habitat (Reinhart et al., 2003; Callaway et al., 2004). Our model predictions are consistent with these observations, in that they imply that established resident communities of coexisting species are more likely to have negative frequency dependence, and such communities are easily invaded by species with mildly positive frequency dependence. However, more importantly our work identifies that the relevant variables are the *relative* signs, magnitudes and spatial scales of the interactions of resident and introduced species in the *target* community, rather than shifts in frequency dependence of introduced species between their native and new habitats. The predictions in this paper are based on several simplifying assumptions such as equal maximum habitat suitabilities for all species, rectangular and equivalent interaction and dispersal neighborhoods, and linear frequency dependence. Future work will consider the effects of frequency dependence on invasiveness under more general conditions.

In summary, frequency dependent interactions can have a big impact on species coexistence and invasiveness, and must be considered to fully understand community dynamics. The spatial scale on which these interactions occur can dramatically affect community structure and population dynamics. Understanding cluster formation and density and the relative local inter-specific dynamics in the interiors, exteriors, and boundaries of self-organizing clusters of con-specifics can provide insights into the mechanisms governing emergence of community-wide spatio-temporal dynamics. Our results also highlight the importance of considering non-equilibrium dynamics, since the time horizon of environmental changes may well be shorter than the time horizon to achieve equilibrium conditions. The model proposed herein provides a theoretical framework for studying frequency dependent interactions that may shed light on spatial and temporal dynamics in real ecological communities.

Acknowledgements

We are grateful to Frédéric Guichard, whose discussions provided insight into our results, and to the editor and two anonymous reviewers for their helpful suggestions. This work was supported in part by a pilot award funded by DOE-FG02-00ER45828 awarded by the US Department of Energy through its EPSCoR Program.

REFERENCES

Ågren, J., 1996. Population size, pollinator limitation and seed set in the self-incompatible herb *Lythrum salicaria*. Ecology 77, 1779–1790.

Balzter, H., Braun, P.W., Köhler, W., 1998. Cellular automata models for vegetation dynamics. Ecol. Model. 107, 113–125.

Bascompte, J., Rodríguez, M.A., 2000. Self-disturbance as a source of spatiotemporal heterogeneity: the case of the tallgrass prairie. J. Theor. Biol 204, 153–164.

Berec, L., 2002. Techniques of spatially explicit individual-based models: construction, simulation, and mean-field analysis. Ecol. Model. 150, 55–81.

Bever, J.D., 1999. Dynamics within mutualism and the maintenance of diversity: inference from a model of interguild frequency dependence. Ecol. Lett. 2, 52–61.
Bever, J.D., 2002. Negative feedback within a mutualism: host-specific growth of mycorrhizal fungi reduces plant benefit. Proc. R. Soc. Biol. B 269, 2595–2601.
Bever, J.D., 2003. Soil community dynamics and the coexistence of competitors: conceptual frameworks and empirical tests. New Phytol. 157, 465–473.
Bever, J.D., Westover, K., Antonovics, J., 1997. Incorporating the soil community into plant population dynamics: the utility of the feedback approach. J. Ecol. 85, 561–573.
Bolker, B.M., Pacala, S.W., 1999. Spatial moment equations for plant competition: understanding spatial strategies and the advantages of short dispersal. Am. Nat. 153 (6), 575–602.
Callaway, R.M., Thelen, G.C., Rodriguez, A., Holben, W.E., 2004. Soil biota and exotic plant invasion. Nature 427, 731–733.
Catovsky, S., Bazzaz, F.A., 2000. The role of resource interactions and seedling regeneration in maintaining a positive feedback in hemlock stands. J. Ecol. 88, 100–112.
Chesson, P., 2000. Mechanisms of maintenance of species diversity. Ann. Rev. Ecol. Syst. 31, 343–366.
Clarke, B., 1969. The evidence for apostatic selection. Heredity 24, 347–352.
Condit, R., Hubbell, S.P., Foster, R.B., 1992. Recruitment near conspecific adults and the maintenance of tree and shrub diversity in a neotropical forest. Am. Nat. 140, 261–286.
Connell, J.H., 1983. On the prevalence and relative importance of interspecific competition: evidence from field experiments. Am. Nat. 122, 661–696.
Czárán, T., Bartha, S., 1992. Spatiotemporal dynamic models of plant populations and communities. TREE 7 (2), 38–42.
Dieckmann, U., Law, R., Metz, J.A.J., 2000. The Geometry of Ecological Interactions. Cambridge University Press, Cambridge, United Kingdom.
Edelstein-Keshet, L., 2005. Mathematical Models in Biology. Society of Industrial and Applied Mathematics, Philadelphia, PA.
Etienne, R., Wertheim, B., Hemerik, L., Schneider, P., Powell, J., 2002. The interaction between dispersal, the Allee effect and scramble competition affects population dynamics. Ecol. Model. 148, 153–168.
Feagin, R.A., Wu, X.B., Smeins, F.E., Whisenant, S.G., Grant, W.E., 2005. Individual versus community level processes and pattern formation in a model of sand dune plant succession. Ecol. Model. 183, 435–449.
Harms, K.E., Wright, S.J., Calderon, O., Hernandez, A., Herre, E.A., 2000. Pervasive density-dependent recruitment enhances seedling diversity in a tropical forest. Nature 404, 493–495.
Herben, T., During, H.J., Law, R., 2000. Spatio-temporal patterns in grassland communities. In: Law, R., Metz, J.A., Dieckmann, U., Metz, H. (Eds.), The Geometry of Ecological Interactions: Simplifying Spatial Complexity. Cambridge University Press, pp. 48–64.
Holley, R.A., Liggett, T.M., 1975. Ergodic theorems for weakly interacting systems and the voter model. Ann. Prob. 3, 643–663.
Holmgren, M., Scheffer, M., Huston, M.A., 1997. The interplay of facilitation and competition in plant communities. Ecology 78, 1966–1975.
Hubbell, S.P., 2001. A Unified Neutral Theory of Biodiversity and Biogeography. Princeton University Press, Princeton University.
Lotka, A.J., 1932. The growth of mixed populations: two species competing for a common food supply. J. Washington Acad. Sci. 22, 461–469.
May, R., Anderson, R.M., 1983. Epidemiology and genetics in the coevolution of parasites and hosts. Proc. R. Soc. Biol. B 219, 281–313.
Molofsky, J., Bever, J.D., 2002. A novel theory to explain species diversity in landscapes: positive frequency dependence and habitat suitability. Proc. R. Soc. Biol. B 269, 2389–2393.
Molofsky, J., Bever, J.D., Antonovics, J., 2001. Coexistence under positive frequency dependence. Proc. R. Soc. Biol. B 268, 273–277.
Molofsky, J., Bever, J.D., Antonovics, J., Newman, T.J., 2002. Negative frequency dependence and the importance of spatial scale. Ecology 83, 21–27.
Murrell, D.J., Purves, D.W., Law, R., 2002. Intraspecific aggregation and species coexistence. Trends Ecol. Evol. 17 (5), 211.
Neuhauser, C., Pacala, S.W., 1999. An explicitly spatial version of the Lotka–Volterra model with interspecific competition. Ann. Appl. Prob. 9, 1226–1259.
Pacala, S.W., Levin, S.A., 1997. Biologically generated spatial pattern and the coexistence of competing species. In: Tilman, D., Kareiva, P. (Eds.), Spatial Ecology. The Role of Space in Population Dynamics and Interspecific Interactions. Princeton University Press, Princeton, New Jersey, pp. 204–232.
Reinhart, K.O., Packer, A., Van der Putten, W.H., Clay, K., 2003. Plant–soil biota interactions and spatial distribution of black cherry in its native and invasive ranges. Ecol. Lett. 6, 1046–1050.
Ronsheim, M.L., 1996. Evidence against a frequency dependent advantage for sexual reproduction in *Allium vineale*. Am. Nat. 147, 718–733.
Ronsheim, M.L., Anderson, S.E., 2001. Population-level specificity in the plant–mycorrhizae association alters intraspecific interactions among neighboring plants. Oecologia 128, 77–84.
Smithson, A., McNair, M.R., 1996. Frequency-dependent selection by pollinators: mechanisms and consequences with regard to behaviour of bumblebees *Bombus terrestris* (L.) (Hymenopetera: Apidae). J. Evol. Biol. 9, 571–588.
Stoll, P., Prati, D., 2001. Intraspecific aggregation alters competitive interactions in experimental plant communities. Ecology 82 (2), 319–327.
Tilman, D., 1982. Resource Competition and Community Structure. Princeton University Press, Princeton, NJ.
Tilman, D., 1994. Competition and bodiversity in spatially structured habitats. Ecology 75, 2–16.
Volterra, V., 1926. Variations and fluctuations of the numbers of individuals in animal species living together. In: Chapman, R.N. (Ed.), Animal Ecology. McGraw Hill, New York (reprinted in 1931).
Wang, J., Kropff, M.J., Lammert, B., Christensen, S., Hansen, P.K., 2003. Using CA model to obtain insight into mechanism of plant population spread in a controllable system: annual weeds as an example. Ecol. Model. 166, 277–286.
Weltzin, J., McPherson, G., 1999. Facilitation of conspecific seedling recruitment and shifts in temperate savanna ecotones. Ecol. Monogr. 69, 513–534.
Westover, K.M., Bever, J.D., 2001. Mechanisms of plant species coexistence: complementary roles of rhizosphere bacteria and root fungal pathogens. Ecology 82, 3285–3294.
Wills, C., Condit, R., 1999. Similar non-random processes maintain diversity in two tropical rainforests. Proc. R. Soc. Biol. B 266, 1445–1452.
Wills, C., Condit, R., Foster, R.B., Hubbell, S.P., 1997. Strong density- and diversity-related effects help to maintain tree species diversity in a neotropical forest. Proc. Nat. Acad. Sci. 94, 1252–1257.

Wilson, J.B., Agnew, A.D.Q., 1992. Positive-feedback switches in plant communities. Adv. Ecol. Res. 23, 263–336.
Wolfe, B.E., Klironomos, J.N., 2005. Breaking new ground: soil communities and exotic plant invasion. Bioscience 55 (6), 477–487.
Wright, S.J., 2002. Plant diversity in tropical forests: a review of mechanisms of species coexistence. Oecologia 130, 1–14.
Wu, J., Marceau, D., 2002. Modeling complex ecological systems: an introduction. Ecol. Model. 153, 1–6.